IEEE Photonics Journal
An IEEE Photonics Society Publication

Open Access

On the Error Probability of Cognitive RF-FSO Relay Networks Over Rayleigh/EW Fading Channels With Primary-Secondary Interference

Volume 12, Number 1, February 2020

Eylem Erdogan, ***Member, IEEE***
Nihat Kabaoglu, ***Member, IEEE***
Ibrahim Altunbas, ***Senior Member, IEEE***
Halim Yanikomeroglu, ***Fellow, IEEE***

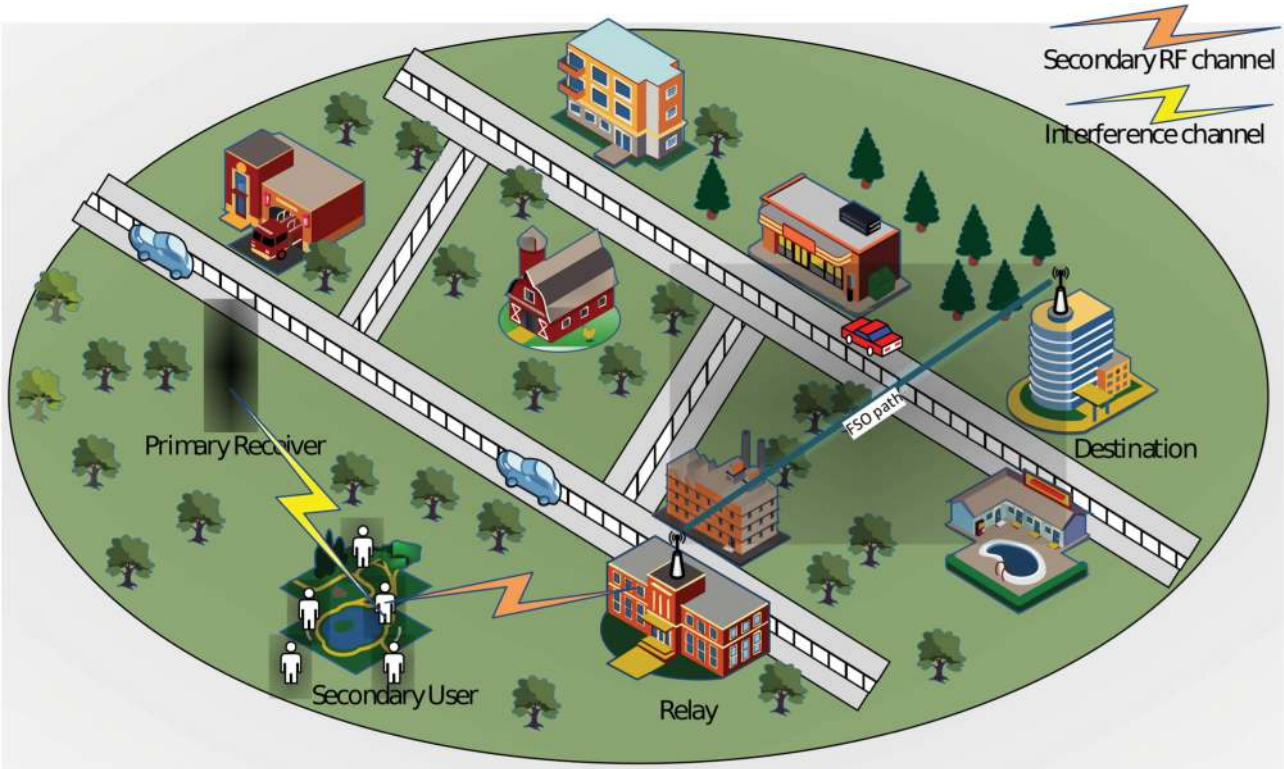

DOI: 10.1109/JPHOT.2019.2955744

IEEE photonics SOCIETY
IEEE

On the Error Probability of Cognitive RF-FSO Relay Networks Over Rayleigh/EW Fading Channels With Primary-Secondary Interference

Eylem Erdogan,[1,2] ***Member, IEEE***, **Nihat Kabaoglu**,[2] ***Member, IEEE***, **Ibrahim Altunbas**,[3] ***Senior Member, IEEE***, **and Halim Yanikomeroglu**,[1] ***Fellow, IEEE***

[1]Department of Systems and Computer Engineering, Carleton University, Ottawa, ON K1S 5B6, Canada
[2]Department of Electrical and Electronics Engineering, Istanbul Medeniyet University, Uskudar, Istanbul 34720, Turkey
[3]Department of Electronics and Communication Engineering, Istanbul Technical University, Maslak, Istanbul 34469, Turkey

DOI:10.1109/JPHOT.2019.2955744

Manuscript received August 25, 2019; revised November 16, 2019; accepted November 21, 2019. Date of publication November 25, 2019; date of current version January 7, 2020. Corresponding author: Eylem Erdogan (e-mail: erdoganeyl@gmail.com).

Abstract: Free space optical (FSO) communication has emerged to provide line of sight connectivity and higher throughput over unlicensed optical spectrums. Cognitive radio (CR), on the other hand, can utilize the radio frequency (RF) spectrum and allow a secondary user (SU) to share the same spectrum with the primary user (PU) as long as the SU does not impose interference on the PU. Owing to the potential of these emerging technologies, to provide full spectrum efficiency, this paper focuses on the mixed CR RF-FSO transmission scheme, where RF communication is employed at one hop followed by the FSO transmission on the other hop in a dual-hop decode-and-forward (DF) configuration. To quantify the performance of the proposed scheme, closed form error probability is derived over Rayleigh/Exponentiated Weibull (EW) fading distributions by considering the statistical and instantaneous feedback channel of the primary network. We also employed an asymptotic analysis to illustrate the diversity gain of the overall system. We believe that the proposed scheme can be applicable to the 5G+ networks where an unlicensed university student connects to the home computer with the aid of an FSO path.

Index Terms: Cognitive radio, free space optical communication, error probability, exponentiated weibull fading.

1. Introduction

Wireless traffic has been increasing at an accelerating rate over the past several years as the number of wireless devices has been proliferating. The increase in wireless devices and overall data traffic poses the problem of spectrum scarcity, which is due to the underutilization of the wireless spectrum [1]. To solve this spectrum utilization problem and to meet the demand for reliable, fast and ubiquitous mobile communication, several promising technologies have recently emerged. Among them, cognitive radio (CR) and free space optical (FSO) communication have attracted considerable interest. CR works by enabling the spectrum sharing paradigm to utilize

the wireless spectrum, whereas FSO provides line of sight connectivity over unlicensed optical spectrums with Gigabit throughput and inherent security.

In CR, a spectrum sharing paradigm is enabled so that an unlicensed user can share the same spectrum with the licensed user [2]. The CR technology can be realized with different spectrum sharing modes. In the underlay mode, which is arguably the most practical, the secondary user (SU) shares the same spectrum with the primary user (PU) as long as the SU related interference remains below a predefined range [3], [4]. To leverage the advantages of CR and to provide reliable communication with utmost coverage for wireless users, relay aided transmission has received considerable attention in recent years [5]. In relay aided transmission, relays can either use amplify-and-forward (AF) or decode-and-forward (DF) protocols to transmit the source signal to the destination node [6]. In the literature, relay aided CR technology has been frequently studied in [7]–[9] and the references therein.

As for FSO systems, these have been shown to alleviate the spectrum utilization problem in wireless systems by providing secure and reliable communication over unlicensed optical spectrums [10], [11]. On account of this potential, FSO systems can be used in campus connectivity, video monitoring, security issues and broadcasting in special events like sports and ceremonies in 5G+ networks [12], [13]. Despite its numerous advantages, the performance of optical wireless communication can be severely degraded by atmospheric turbulence induced fading, which can be modeled with Gamma-Gamma (GG), Log-normal, $\mathcal{K}$ and Exponentiated Weibull (EW) fading channels, depending on the severity of the atmospheric turbulence [14]. For example, Log-normal is used for weak turbulence affects, $\mathcal{K}$ can model strong atmospheric conditions and GG can be used for specific aperture sizes. Unlike these models, EW fading can be adopted in all atmospheric weather conditions along with various aperture sizes [15], [16].

To reduce the severe effects of turbulence and to address the problem of last mile connectivity in backbone networks, FSO systems can be employed with an RF counterpart in a dual-hop configuration. The so-called mixed RF-FSO communication can reap the advantages of FSO systems while dealing with the atmospheric turbulence induced fading. Due to this potential, there has been a growing interest in mixed RF-FSO systems in the literature. Specifically, [17] and [18] considered mixed RF-FSO systems for variable AF relaying where important system parameters including outage probability (OP) and error probability (EP) were derived for GG and $\mathcal{M}$ fading channels, respectively. Most recently, [19] elaborated the hybrid DF RF-FSO relaying for supporting mobile communication, [20] investigated DF RF-FSO relaying and performed precise analyses for modulation-detection schemes including heterodyne detection and intensity modulation-direct detection. Moreover, DF and AF RF-FSO relaying schemes were also considered for EW fading channels in [21]–[23] and the references therein.

Another line of research in mixed RF-FSO systems has focused on mixed CR RF-FSO transmission. In CR RF-FSO transmission, a secondary source node working in the underlay mode seeks to transmit information to the destination node with the aid of an optical path connected to the backbone network. For this set-up, [24] investigated the DF CR RF-FSO scheme where outage probability was obtained and diversity analysis was conducted for Nakagami-*m*/GG fading channels, whereas [25] and [26] investigated the MIMO CR RF-FSO relaying where various diversity techniques were enabled at the RF path, and important system indicators were obtained in the presence of practical channel imperfections like nodes mobility. Moreover, [27] considered different interference cancellation techniques at the RF side for the AF CR RF-FSO scheme and derived outage probability for Rayleigh/GG fading. Finally, [28] was investigated DF CR RF-FSO relaying for Nakagami-*m*/EW fading channels where outage probability and ergodic capacity were derived for a mean-value power allocation scheme without considering the instantaneous interference channel of the primary network (PN).

1.1 Motivation and Contributions

As the aforementioned studies show, the current literature is limited with regard to GG fading at the FSO path, and almost all existing works have focused on the outage probability analysis as

TABLE 1
Literature About CR RF-FSO Systems

Ref.	System Model	RF Link	FSO Link	Interference	Performance Metrics
[24]	AF	Nakagami-m	GG	Instantaneous	Outage Probability
[25]	MIMO DF	Rayleigh	GG	Instantaneous	Outage, Error Probability
[26]	MIMO DF	Nakagami-m	GG	Instantaneous	Outage Probability
[27]	MIMO AF	Rayleigh	GG	Instantaneous	Outage Probability
[28]	DF	Nakagami-m	EW	Statistical	Outage Probability, Ergodic Capacity

shown in Table 1. Specifically, [25] considered only GG fading channel and provided a simple analysis for the asymptotic error floor by considering only CR RF transmission and hence, the authors neglected the impact of the FSO path. On the other hand, [24], [26]–[28] studied the outage probability performance of the CR RF-FSO scheme without considering the error probability analysis. Moreover, primary-secondary interference has not been considered in the aforementioned works, and none of them have studied both instantaneous and statistical power allocation methods together for the CR RF-FSO scheme. Motivated by the wide use of the RF-FSO scheme and to fill in the gap in the literature, we considered a DF RF-FSO scheme for Rayleigh/EW fading model where EP expressions are obtained by considering both the statistical and instantaneous feedback channel of the PN. The contributions of this paper can be summarized as follows:

- First time in the literature, we considered CR RF-FSO relaying over Rayleigh/EW fading channels, where a tractable closed-form EP expression was obtained considering both statistical and instantaneous feedback channel of the PN. The results show that instantaneous power allocation slightly outperforms in the low SNR regime.
- To present further insight about the impact of RF and FSO system parameters, we investigated the overall diversity of the proposed scheme by pursuing asymptotic EP analysis. High SNR analysis shows that the overall diversity of the CR RF-FSO scheme depends on both optical and RF fading severity, and it is independent from the PN.
- Different from the CR RF-FSO literature, the impact of primary-secondary interference on the secondary network was investigated and EP was derived. Please note that, almost all the works in the current literature have neglected the primary-secondary interference, which can be crucial for the performance of the secondary network.

2. Signal and System Model

In this section, we consider a dual-hop underlay RF-FSO network, where a secondary source S seeks to communicate with a destination D over a relay terminal R in two phases. We assume that the direct path between S and D is not available due to non line-of-sight connectivity. It is important to mention that the proposed underlay RF-FSO architecture can remedy the problem of spectrum utilization in wireless systems. More precisely, CR technology can utilize the spectrum at the RF side while FSO allows license free spectrum with Gigabit data rates.

In this way, the proposed scheme, which is drawn in Fig. 1, can be viable for 5G+ networks, where an unlicensed university student (user) attempts to communicate with a destination node like a home computer over an FSO path in the backbone network. This figure illustrates that a secondary user is working in the underlay fashion without causing any interference to the primary base station. In the meanwhile, the FSO transceiver, deployed at the rooftop of the buildings, transferring the source information to the destination node. The following subsections present cognitive RF and FSO transmissions respectively.

2.1 Cognitive RF Transmission

In the underlay RF transmission, S transmits its information to R while adhering the interference power constraints of the (PN). In this process, the, the transmit power at S is set to $P_S = \min(Q_p/|h_{S,P}|^2, P_{\max})$ [7], where Q_p is the maximum tolerable interference power, $h_{S,P}$ is the

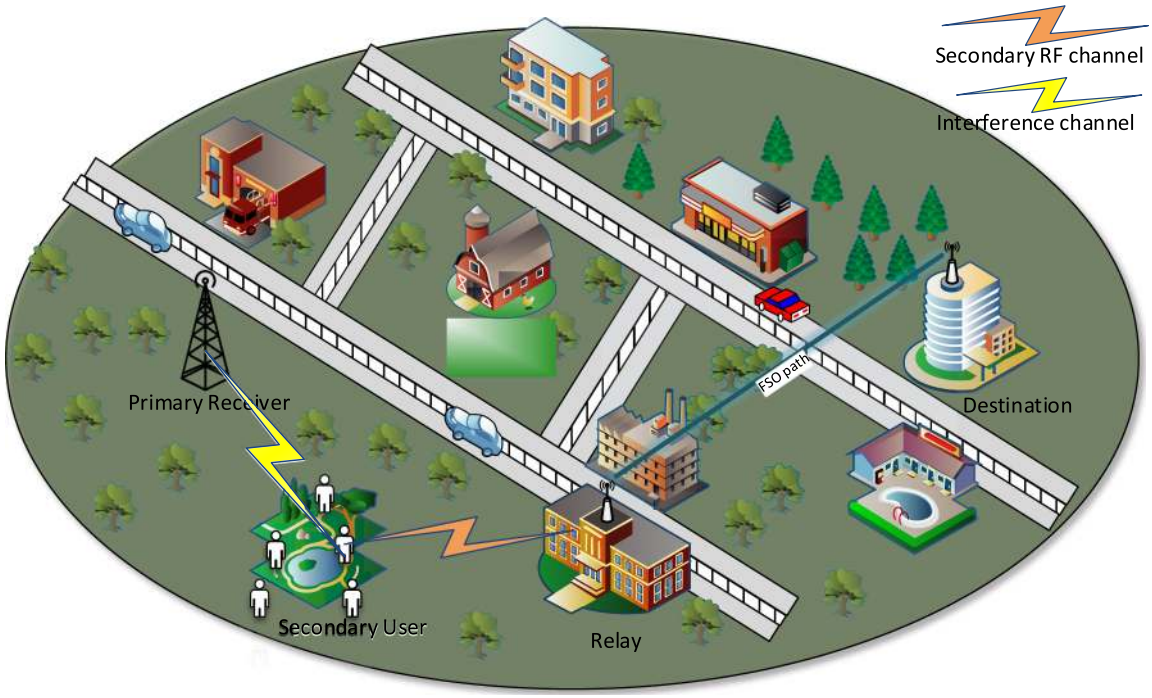

Fig. 1. Illustration of the CR RF-FSO relaying scheme where an unlicensed user connects to the destination node over the FSO path without causing interference to the primary network.

RF interference channel between S and primary receiver P and $P_{\max}$ is the maximum available power in the secondary network. To simplify the analysis, S can be taken as a stationary station with unlimited power, e.g., $P_{\max} \to \infty$ [29]. In this case, P_S can be given as $P_S = Q_p/|h_{S,P}|^2$. Following the interference limitations of the PN, the received signal at R can be expressed as

$$y_{S,R} = \sqrt{Q_P/|h_{S,P}|^2}\, h_{S,R} x_S + n_R, \tag{1}$$

where $h_{S,R}$ is the channel coefficient between $S \to R$ path, n_R is the additive white Gaussian with N_0 one sided power spectral density, and x_S is the source signal.

2.2 FSO Transmission

In the second phase, R first uses a band-pass filter to remove the DC components of the received signal. Next, it detects the source signal, modulates it with binary phase shift keying (BPSK) modulation, and forwards it to destination after proper biasing. At D, the photocurrent converts the optical signal to an electrical one, and the received signal can be written as

$$y_{R,D} = \zeta \sqrt{P_R} I_{R,D} \bar{x}_S + n_D, \tag{2}$$

where $\bar{x}_S$ is the detected source signal at R, n_D is the additive white Gaussian with N_0 one sided power spectral density, $I_{R,D}$ is optical channel gain, $0 \leq \zeta \leq 1$ is the electrical-optical conversion ratio, and P_R is the relay power. In DF relaying, the end-to-end instantaneous SNR can be expressed as

$$\gamma_{e2e} = \min\left(\gamma_{S,R}, \gamma_{R,D}\right), \tag{3}$$

where $\gamma_{S,R} = \frac{Q_P}{N_0} \frac{|h_{S,R}|^2}{|h_{S,P}|^2}$ and $\gamma_{R,D} = \zeta^2 P_R \frac{I_{R,D}^2}{N_0}$.

3. Statistical Properties of the Fading Channels

3.1 Fading Statistics of the Underlay RF Channel

In this section, we assume that $S \rightarrow R$ and $S \rightarrow P$ paths follow Rayleigh distribution. In the underlay paradigm, the CDF of $\gamma_{S,R}$ can be expressed as [30]

$$F_{\gamma_{S,R}}(\gamma) = \int_0^{\infty} F_{|h_{S,R}|^2}\left(\frac{x\gamma}{\varpi}\right) f_{|h_{S,P}|^2}(x)dx, \tag{4}$$

where $\varpi = \frac{Q_P}{N_0}$ is the average SNR of the first hop, $F_{|h_{S,R}|^2}(x)$ is the cumulative distribution function (CDF) of $|h_{S,R}|^2$ and $f_{|h_{S,P}|^2}(x)$ is the probability density function (PDF) of $|h_{S,P}|^2$. As both $S \rightarrow R$ and $S \rightarrow P$ paths are modeled with Rayleigh fading, the $F_{|h_{S,R}|^2}(\frac{x\gamma}{\varpi})$ and, $f_{|h_{S,P}|^2}(x)$ can be given as

$$F_{|h_{S,R}|^2}\left(\frac{x\gamma}{\varpi}\right) = 1 - \exp\left(-\frac{x\gamma}{\varpi}\right)$$
$$f_{|h_{S,P}|^2}(x) = \exp(-x). \tag{5}$$

By substituting (5) into (4), $F_{\gamma_{S,R}}(\gamma)$ can be expressed as [31]

$$F_{\gamma_{S,R}}(\gamma) = 1 - \frac{1}{1+\gamma/\varpi}. \tag{6}$$

3.2 Fading Statistics of the FSO Channel

As the FSO path is modeled with EW fading, PDF and CDF of the $R \rightarrow D$ path can be written as [15], [16]

$$f_{h_{R,D}}(I) = \frac{\alpha\beta}{\eta}\left(\frac{I}{\eta}\right)^{\beta-1} \exp\left[-\left(\frac{I}{\eta}\right)^{\beta}\right]\left(1-\exp\left[-\left(\frac{I}{\eta}\right)^{\beta}\right]\right)^{\alpha-1}, I > 0 \tag{7}$$

and

$$F_{h_{R,D}}(I) = \left(1-\exp\left[-\left(\frac{I}{\eta}\right)^{\beta}\right]\right)^{\alpha}, \tag{8}$$

where α, β are the shape parameters and η is the scale parameter. With the aid of [32], the CDF of $\gamma_{R,D}$ can be given as

$$F_{\gamma_{R,D}}(\gamma) = \sum_{\rho=0}^{\infty}\binom{\alpha}{\rho}(-1)^{\rho}\exp\left[-\rho\left(\frac{\gamma}{\eta^2\bar{\gamma}_{R,D}}\right)^{\frac{\beta}{2}}\right], \tag{9}$$

where $\bar{\gamma}_{R,D} = \zeta^2\frac{P_R}{N_0}$ is the average SNR of the $R \rightarrow D$ path. With the aid of (3), the CDF of e2e SNR can be expressed as

$$F_{\gamma_{e2e}(\gamma)} = F_{\gamma_{S,R}}(\gamma) + F_{\gamma_{R,D}}(\gamma) - F_{\gamma_{S,R}}(\gamma)F_{\gamma_{R,D}}(\gamma), \tag{10}$$

and $F_{\gamma_{e2e}}(\gamma)$ can be obtained easily by substituting (6) and (9) into (10).

4. Error Probability Analysis

Error probability (EP) is one of the most important performance indicators in wireless systems, and it can reveal a lot about the nature of the system behavior. EP can be represented by the following generic formula [33] for many modulation formats including coherent and differential BPSK as

$$P_s(e) = \frac{\varphi^p}{2\Gamma(p)}\int_0^{\infty}\gamma^{p-1}\exp[-\varphi\gamma]F_{\gamma_{e2e}}(\gamma)d\gamma, \tag{11}$$

TABLE 2
Modulation Parameters

Modulation	p	φ
Coherent binary phase shift keying (CBPSK)	0.5	1
Coherent binary frequency shift keying (CBFSK)	0.5	0.5
Non-coherent binary frequency shift keying (NBFSK)	1	0.5
Differential binary phase shift keying (DBPSK)	1	1

where p and φ are parameters related to different modulation types, which are given in Table 2, and $\Gamma(\cdot)$ denotes the Gamma function [34, eqn. (8.339.1)].

4.1 Closed-Form Error Probability Analysis

Here, we first need to find a closed form EP expression. To do so, we substitute (6) and (9) into (11) and obtain $P_s(e)$ as

$$P_s(e) = \underbrace{\frac{\varphi^p}{2\Gamma(p)}\int_0^\infty \gamma^{p-1}\exp[-\varphi\gamma]\left(1-\frac{1}{1+\gamma/\varpi}\right)d\gamma}_{\mathcal{I}_1} + \underbrace{\frac{\varphi^p}{2\Gamma(p)}\sum_{\rho=0}^{\infty}\binom{\alpha}{\rho}(-1)^\rho\int_0^\infty \gamma^{p-1}\exp[-\varphi\gamma]\exp\left[-\rho\left(\frac{\gamma}{\eta^2\bar{\gamma}_{R,D}}\right)^{\frac{\beta}{2}}\right]d\gamma}_{\mathcal{I}_2} - \underbrace{\frac{\varphi^p}{2\Gamma(p)}\sum_{\rho=0}^{\infty}\binom{\alpha}{\rho}(-1)^\rho\int_0^\infty \gamma^{p-1}\exp[-\varphi\gamma]\left(1-\frac{1}{1+\gamma/\varpi}\right)\exp\left[-\rho\left(\frac{\gamma}{\eta^2\bar{\gamma}_{R,D}}\right)^{\frac{\beta}{2}}\right]d\gamma}_{\mathcal{I}_3}. \tag{12}$$

Thereby, it can be expressed as

$$P_s(e) = \mathcal{I}_1 + \mathcal{I}_2 - \mathcal{I}_3. \tag{13}$$

Next, we derive $\mathcal{I}_1$, $\mathcal{I}_2$ and $\mathcal{I}_3$.

4.1.1 Derivation of $\mathcal{I}_1$: We first invoke the expression $(1-\frac{1}{1+\gamma/\varpi}) = \frac{\gamma}{\varpi+\gamma}$ into $\mathcal{I}_1$ and obtain

$$\mathcal{I}_1 = \frac{\varphi^p}{2\Gamma(p)}\int_0^\infty \gamma^p\exp[-\varphi\gamma]\left(\frac{1}{\varpi+\gamma}\right)d\gamma. \tag{14}$$

Then, with the aid of [34, eqn. (3.383.10)], $\mathcal{I}_1$ can be obtained as

$$\mathcal{I}_1 = \frac{p}{2}\left(\varpi\varphi\right)^p\exp\left[\varpi\varphi\right]\Gamma\left[-p,\varpi\varphi\right], \tag{15}$$

where $\Gamma[\cdot,\cdot]$ denotes the incomplete Gamma function [34, eqn. (8.350.1)].

4.1.2 Derivation of $\mathcal{I}_2$: We first express $\mathcal{I}_2$ as

$$\mathcal{I}_2 = \frac{\varphi^p}{2\Gamma(p)}\sum_{\rho=0}^{\infty}\binom{\alpha}{\rho}(-1)^\rho\int_0^\infty \gamma^{p-1}\exp[-\varphi\gamma]\exp\left[-\rho\left(\frac{\gamma}{\eta^2\bar{\gamma}_{R,D}}\right)^{\frac{\beta}{2}}\right]d\gamma. \tag{16}$$

Then, we invoke $\exp[-\varphi\gamma] = G_{0,1}^{1,0}[\varphi\gamma|\begin{smallmatrix}-\\0\end{smallmatrix}]$ [35, eqn. (01.03.26.0004.01)] into $\mathcal{I}_2$ as

$$\mathcal{I}_2 = \frac{\varphi^p}{2\Gamma(p)}\sum_{\rho=0}^{\infty}\binom{\alpha}{\rho}(-1)^\rho\int_0^\infty \gamma^{p-1}G_{0,1}^{1,0}\left[\varphi\gamma\middle|\begin{matrix}-\\0\end{matrix}\right]\exp\left[-\rho\left(\frac{\gamma}{\eta^2\bar{\gamma}_{R,D}}\right)^{\frac{\beta}{2}}\right]d\gamma. \tag{17}$$

Then, by applying the transformation $x = \rho(\frac{1}{\eta^2\bar{\gamma}_{R,D}})^{\frac{\beta}{2}}\gamma^{\beta/2}$ into (17), with the aid of $\exp[-x] = G_{0,1}^{1,0}[x|\overline{0}]$, we obtain

$$\mathcal{I}_2 = \frac{\varphi^p}{\beta\Gamma(p)}\sum_{\rho=0}^{\infty}\binom{\alpha}{\rho}(-1)^{\rho}\left(\frac{\eta^2\bar{\gamma}_{R,D}}{\rho^{2/\beta}}\right)^{p}\int_0^{\infty}x^{\frac{2}{\beta}p-1}G_{0,1}^{1,0}\left[\varphi\left(\frac{\eta^2\bar{\gamma}_{R,D}}{\rho^{2/\beta}}\right)x^{2/\beta}\middle|\overline{0}\right]G_{0,1}^{1,0}\left[x\middle|\overline{0}\right]dx, \tag{18}$$

and the above integral can be obtained by using [35, eqn. (07.34.21.0012.01)] as

$$\mathcal{I}_2 = \frac{\varphi^p}{\beta\Gamma(p)}\sum_{\rho=0}^{\infty}\binom{\alpha}{\rho}(-1)^{\rho}\left(\frac{\eta^2\bar{\gamma}_{R,D}}{\rho^{2/\beta}}\right)^{p}\mathcal{H}_{1,1}^{1,1}\left[\varphi\left(\frac{\eta^2\bar{\gamma}_{R,D}}{\rho^{2/\beta}}\right)\middle|\begin{matrix}\left(1-\frac{2p}{\beta},\frac{2}{\beta}\right)\\(0,1)\end{matrix}\right], \tag{19}$$

where $\mathcal{H}_{a,b}^{c,d}[\cdot|\cdot]$ denotes the Fox-H function [36].

4.1.3 Derivation of $\mathcal{I}_3$: It is important to mention that $\mathcal{I}_3$ can not be evaluated in a closed form solution to the best of our knowledge. However, an approximate result can be obtained by applying some theoretical manipulations. First, we express $(1-\frac{1}{1+\gamma/\varpi}) = \frac{\gamma}{\varpi}(1+\frac{\gamma}{\varpi})^{-1}$. Then, by using the observation of $(1+\frac{\gamma}{\varpi})^{-1} \approx 1-\frac{\gamma}{\varpi}$ in $\mathcal{I}_3$, we can express it in a more tractable form as

$$\mathcal{I}_3 = \frac{\varphi^p}{2\varpi\,\Gamma(p)}\sum_{\rho=0}^{\infty}\binom{\alpha}{\rho}(-1)^{\rho}\int_0^{\infty}\gamma^p\exp[-\varphi\gamma]\exp\left[-\rho\left(\frac{\gamma}{\eta^2\bar{\gamma}_{R,D}}\right)^{\frac{\beta}{2}}\right]d\gamma$$
$$-\frac{\varphi^p}{2\varpi^2\Gamma(p)}\sum_{\rho=0}^{\infty}\binom{\alpha}{\rho}(-1)^{\rho}\int_0^{\infty}\gamma^{p+1}\exp[-\varphi\gamma]\exp\left[-\rho\left(\frac{\gamma}{\eta^2\bar{\gamma}_{R,D}}\right)^{\frac{\beta}{2}}\right]d\gamma. \tag{20}$$

Hence, the closed form solution of the above integral can be easily obtained as given in Section 4.1.2. It is also worth noting that at medium and high SNRs, $\mathcal{I}_3 \to 0$ [37]. Thereby, $P_s(e)$ can be approximately written as

$$P_s(e) \approx \mathcal{I}_1 + \mathcal{I}_2. \tag{21}$$

4.2 Asymptotic Error Probability Analysis

At high SNR, the EP can be expressed as

$$P_s^{\infty}(e) = \underbrace{\frac{\varphi^p}{2\Gamma(p)}\int_0^{\infty}\gamma^{p-1}\exp[-\varphi\gamma]\mathcal{F}_{\gamma_{S,R}}^{\infty}(\gamma)d\gamma}_{\mathcal{I}_4} + \underbrace{\frac{\varphi^p}{2\Gamma(p)}\int_0^{\infty}\gamma^{p-1}\exp[-\varphi\gamma]\mathcal{F}_{\gamma_{R,D}}^{\infty}(\gamma)d\gamma}_{\mathcal{I}_5}. \tag{22}$$

Invoking the Taylor series expansion of $(1+t)^{-a} = 1-at+\cdots+\frac{a(a+1)\cdots(a+n-1)}{n!}t^n$ into $\mathcal{I}_4$, then by substituting the high SNR assumption of $\exp(-x/a) \approx 1-x/a$ into $\mathcal{I}_5$ and after omitting the small valued terms, we obtain $P_s^{\infty}(e)$ as

$$P_s^{\infty}(e) = \frac{\varphi^p}{2\Gamma(p)}\int_0^{\infty}\gamma^{p-1}\exp[-\varphi\gamma]\left(\frac{\gamma}{\varpi}\right)d\gamma + \frac{\varphi^p}{2\Gamma(p)}\int_0^{\infty}\gamma^{p-1}\exp[-\varphi\gamma]\left(\frac{1}{\eta}\sqrt{\frac{\gamma}{\bar{\gamma}_{R,D}}}\right)^{\alpha\beta}d\gamma. \tag{23}$$

By evaluating the above integral with the aid of [34, eqn. (3.381.4)], $P_s^{\infty}(e)$ can be obtained as

$$P_s^{\infty}(e) = \frac{p}{2\varphi\varpi} + \frac{\Gamma\left(p+\frac{\alpha\beta}{2}\right)\varphi^{-\alpha\beta/2}}{2\Gamma(p)(\eta^2\bar{\gamma}_{R,D})^{\alpha\beta/2}}. \tag{24}$$

If we assume $\bar{\gamma} = \kappa_1 \varpi = \kappa_2 \bar{\gamma}_{R,D}$, where κ_1 and κ_2 are positive constants, we obtain $P_s^{\infty}(e)$ as

$$P_s^{\infty}(e) = \frac{\mathcal{A}}{2}\left(\frac{1}{\bar{\gamma}}\right)^{\min(1,\alpha\beta/2)}, \tag{25}$$

where $\mathcal{A}$ is

$$\mathcal{A} = \begin{cases} \frac{\kappa_1 p}{2\varphi}, & 1 < \alpha\beta/2 \\ \frac{\kappa_1 p}{2\varphi} + \frac{\kappa_2 \Gamma\left(p+\frac{\alpha\beta}{2}\right)\varphi^{-\alpha\beta/2}}{2\Gamma(p)(\eta)^{\alpha\beta}} & 1 = \alpha\beta/2 \\ \frac{\kappa_2 \Gamma\left(p+\frac{\alpha\beta}{2}\right)\varphi^{-\alpha\beta/2}}{2\Gamma(p)(\eta)^{\alpha\beta}}, & 1 > \alpha\beta/2. \end{cases} \tag{26}$$

The above expression shows that the overall diversity gain of the proposed scheme is $\mathcal{G}_d = \min(1, \alpha\beta/2)$. It is important to note that $\alpha\beta/2 < 1$ in the presence of high turbulence fading for point-like apertures.

4.3 Error Probability Analysis in the Presence of Limited Feedback

In underlay CR networks, the transmit power is given as $P_S = Q_p/|h_{S,P}|^2$ to adhere to interference power limitations of the PU, as described in Section 2.1. However, this approach may not be practical when $h_{S,P}$ varies rapidly, and in some circumstances it may present a huge feedback burden as it is hard to know the instantaneous feedback gain. To lower the feedback burden and prevent feedback errors, mean-value (MV) power allocation (also known as limited feedback), which uses the MV of the feedback gain, can be adopted in CR networks [38]. In MV power allocation, the transmit power at S can be written as $P_S = \min(Q_p/E[|h_{S,P}|^2], P_{\max})$, where $E[\cdot]$ denotes the expectation operator and $P_{\max}$ is the maximal available power in the secondary network. It is important to note that $\bar{Q}_p = Q_p/N_0$ and $\bar{P}_{\max} = P_{\max}/N_0$. In this regard, the CDF of $\gamma_{S,R}$ can be expressed as

$$F_{\gamma_{S,R}}^{\mathrm{LF}}(\gamma) = 1 - \exp\left[-\frac{\gamma}{\min(\bar{Q}_p/E[|h_{S,P}|^2], \bar{P}_{\max})}\right]. \tag{27}$$

By substituting $F_{\gamma_{S,R}}^{\mathrm{LF}}(\gamma)$ into $\mathcal{I}_1$, with a few manipulations, we obtain

$$\mathcal{I}_1^{\mathrm{LF}} = \frac{1}{2} - \frac{\varphi^p}{2\Gamma(p)}\int_0^{\infty} \gamma^{p-1}\exp[-\varphi\gamma]\exp\left[-\frac{\gamma}{\min(\bar{Q}_p/E[|h_{S,P}|^2], \bar{P}_{\max})}\right]d\gamma. \tag{28}$$

With the aid of [34, eqn. (3.381.4)], the above expression can be given as

$$\mathcal{I}_1^{\mathrm{LF}} = \frac{1}{2} - \frac{\varphi^p}{2}\left(\frac{1}{\min(\bar{Q}_p/E[|h_{S,P}|^2], \bar{P}_{\max})} + \varphi\right)^{-p}. \tag{29}$$

and EP in the presence of limited feedback can be obtained by substituting (29) and (19) into (21).

4.4 Error Probability Analysis in the Presence of Primary-Secondary Interference

In CR networks, the interference caused by the secondary network can be mitigated by applying appropriate power allocation schemes. However, the secondary communication can be severely affected by the primary interference. In this section, we investigate the impact of primary-secondary interference on the secondary network by considering statistical power allocation, and derive effective EP. In the presence of primary-secondary interference, the signal-to-interference-noise

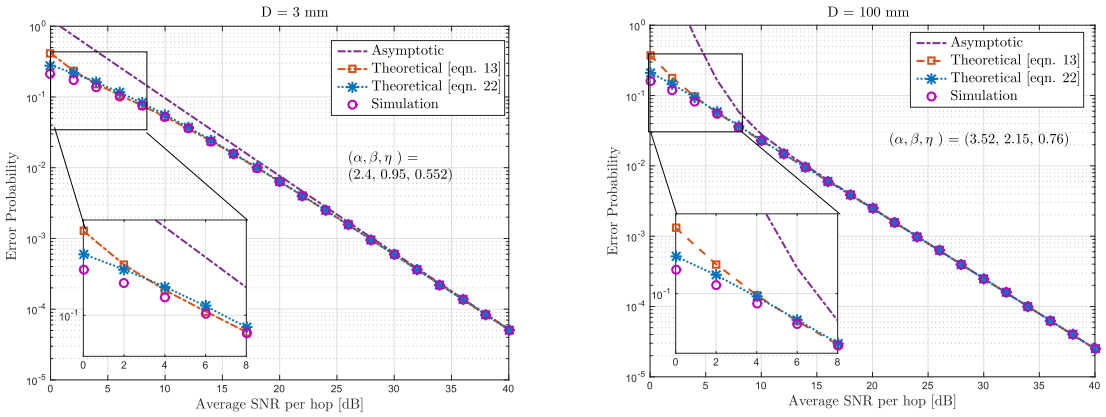

(a) D = 3 mm (b) D = 100 mm

Fig. 2. Error probability performance of the proposed network for instantaneous feedback channel under moderate turbulence conditions.

ratio (SINR) at the $S \rightarrow R$ path can be expressed as

$$\gamma_{S,R}^{\text{ef}} = \frac{\gamma_{S,R}}{1+\gamma_I}, \tag{30}$$

where $\gamma_{S,R} = \min(\bar{Q}_p/E[|h_{S,P}|^2], \bar{P}_{\max})|h_{S,R}|^2$ and $\gamma_I = \frac{P_I}{N_0}|h_I|^2$ is the interference caused by the PN. Please note that P_I is the power of the PN and h_I is the Rayleigh distributed interference channel between the primary transmitter and R. With the aid of [39], the CDF of $\gamma_{S,R}^{\text{ef}}$ can be expressed as

$$F_{\gamma_{S,R}^{\text{ef}}}(\gamma) = \int_0^\infty F_{\gamma_{S,R}}^{\text{LF}}((x+1)\gamma) f_{\gamma_I}(x) dx, \tag{31}$$

where $f_{\gamma_I}(\gamma) = \frac{1}{\bar{\gamma}_I} \exp[-\gamma/\bar{\gamma}_I]$. By invoking $f_{\gamma_I}(\gamma)$ and (27) into the above expression, after a few manipulations, $F_{\gamma_{S,R}^{\text{ef}}}(\gamma)$ can be given as

$$F_{\gamma_{S,R}^{\text{ef}}}(\gamma) = 1 - \frac{\bar{\gamma}_{S,R}^{\text{LF}}}{\gamma\bar{\gamma}_I + \bar{\gamma}_{S,R}^{\text{LF}}} \exp[-\gamma/\bar{\gamma}_{S,R}^{\text{LF}}], \tag{32}$$

where $\bar{\gamma}_{S,R}^{\text{LF}} = \min(\bar{Q}_p/E[|h_{S,P}|^2], \bar{P}_{\max})$. By inserting $F_{\gamma_{S,R}^{\text{ef}}}(\gamma)$ into (11), with the aid of (12) and [34, eqn. (3.383.10)], $\mathcal{I}_1$ can be given as

$$\mathcal{I}_1^{\text{ef}} = \frac{1}{2} - \left(\frac{\varphi^p}{2}\right)\left(\frac{\bar{\gamma}_{S,R}^{\text{LF}}}{\bar{\gamma}_I}\right)^p \exp\left[\frac{\bar{\gamma}_{S,R}^{\text{LF}}}{\bar{\gamma}_I}\left(\varphi + \frac{1}{\bar{\gamma}_{S,R}^{\text{LF}}}\right)\right]\Gamma\left(1-p, \frac{\bar{\gamma}_{S,R}^{\text{LF}}}{\bar{\gamma}_I}\left(\varphi + \frac{1}{\bar{\gamma}_{S,R}^{\text{LF}}}\right)\right), \tag{33}$$

and overall EP can be obtained with the aid of (13) or (21).

5. Numerical Results and Discussion

In this section, the theoretical results are validated with the aid of simulations for various performance criteria. In the simulations, EP figures are depicted for various aperture sizes (D), including $D = 3$ mm, 100 mm and 200 mm's for CBPSK modulation under weak, moderate, and strong turbulence conditions. In all figures, we assume that $\varpi = \bar{\gamma}_{R,D} = \bar{\gamma}$ and $\zeta = 1$ for notational brevity, without losing generality.

Fig. 2a and 2b show the EP performance of the proposed scheme for instantaneous feedback channel in the presence of moderate turbulence fading by considering two different aperture sizes.

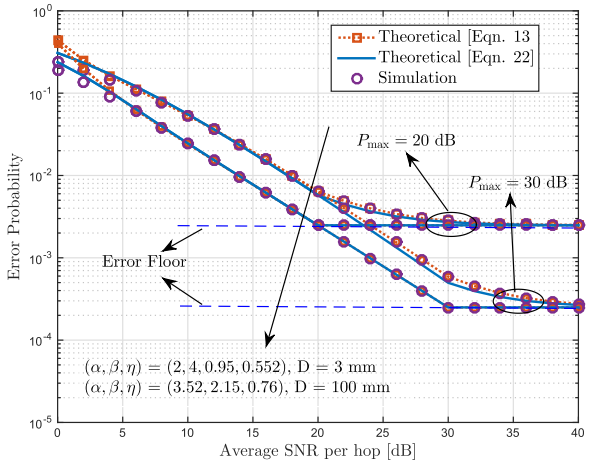

Fig. 3. Error probability performance of the proposed network for instantaneous feedback channel under moderate turbulence conditions.

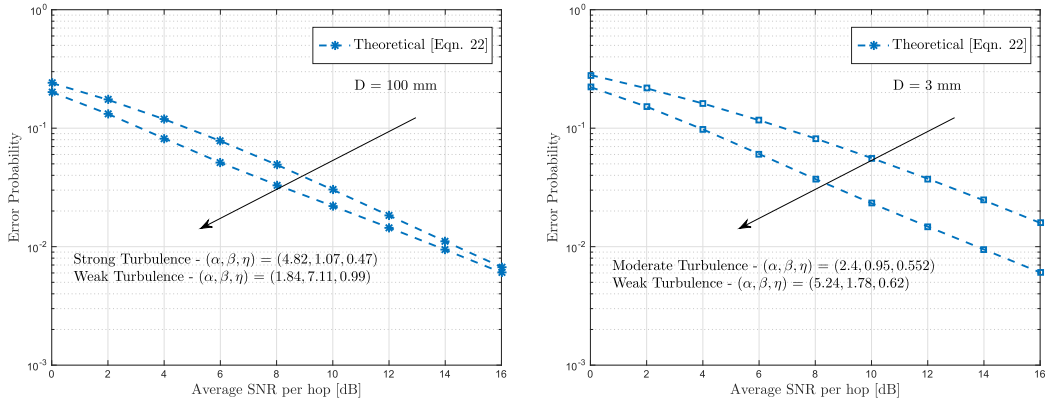

(a) D = 100 mm (b) D = 3 mm

Fig. 4. Error probability performance of the proposed network for instantaneous feedback channel under weak and strong turbulence conditions.

From the figures, we can understand that the theoretical results (eqn. (13) and (21)) are in good agreement with the simulation. Moreover, the magnified figures on the bottom left of Fig. 2a and 2b show that the curves obtained from (13) quickly overlap with the simulation, whereas the curves obtained from (21) perform like a tight upper bound at low and medium SNRs.

Fig. 3 shows the performance of the limited feedback channel in the presence of moderate turbulence fading. We can also see that after the maximum available power ($P_{\max}$) is reached, error floors occur and the diversity goes to zero. Moreover, we note that there is no diversity gain between $D = 3$ mm and $D = 100$ mm curves; this is because the RF side limits the maximum available diversity to 1 due to non-LOS (NLOS) conditions, and the EP difference between two curves is about 5 dB.

Fig. 4a and 4b demonstrate the performance of the proposed scheme for strong and weak turbulence conditions. We can see from the figures that the difference between strong and weak turbulence conditions is almost 0.5 dB at 5×10^{-2} EP when $D = 100$ mm. On the other hand, the difference between both curves increases to 4 dB when when a point-like aperture ($D = 3$ mm) is used at the destination.

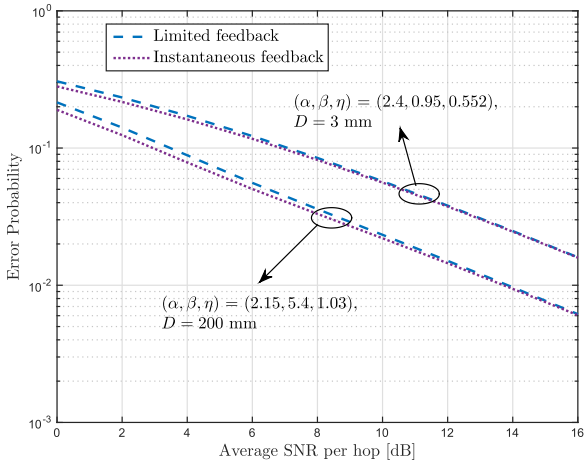

Fig. 5. Error probability comparison of instantaneous and limited feedback channels for various aperture sizes when $P_{\max} = \infty$.

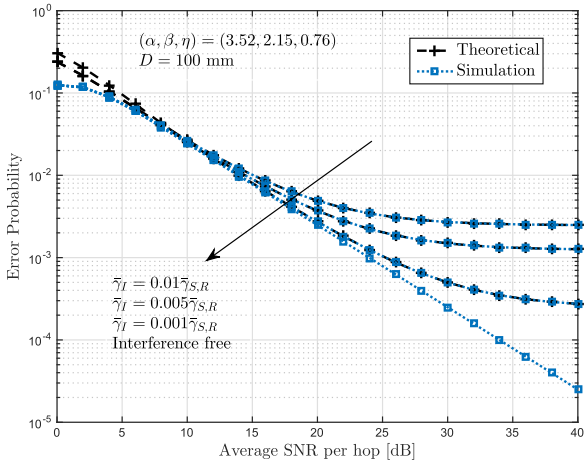

Fig. 6. Impact of primary-secondary interference on the error probability performance of the proposed network for moderate turbulence conditions and $P_{\max} = \infty$.

In Fig. 5, EP performance of the proposed scheme is depicted for limited feedback and instantaneous feedback channels under moderate fading conditions. We observe from the figure that limited feedback and perfect feedback channels achieve the same EP performances at medium and high SNRs. However, the instantaneous feedback channel slightly outperforms to the limited feedback in the low SNR regime.

In Fig. 6, the impact of primary-secondary interference is depicted for the proposed scheme by considering a limited feedback channel. We can see from the figure that the increase in the primary-secondary interference SNR ($\bar{\gamma}_I$) leads to error floors especially at the high SNR regime; this is because the impact of interference becomes dominant compared to the white noise. Moreover, the impact of primary-secondary interference enhances as $\bar{\gamma}_I \to \bar{\gamma}_{S,R}$.

5.1 Design Guidelines

In this section, we illustrate some important guidelines that can be used in the design of practical CR RF-FSO systems.

- Fig. 4 proves that the limited feedback channel can be preferable in the design of practical CR RF-FSO systems as it is easy to obtain the mean-value of the feedback channel and as it can reduce the feedback errors.
- As the RF hop is modeled with Rayleigh fading channel due to NLOS channel conditions, keeping the receive aperture size around 50 mm can be a cost-effective solution for CR RF-FSO systems to cope with the turbulence induced fading without losing EP performance.
- The primary-secondary interference can be crucial for CR RF-FSO systems, as we can see in Fig. 6. To reduce the effects of primary-secondary interference, the relay, which is closer to the source node can be used in the transmission.

6. Conclusion

This paper has focused on the mixed underlay RF-FSO transmission, where RF communication is employed at one hop followed by the FSO transmission on the other hop in a dual-hop decode-and-forward configuration to provide full spectrum efficiency. To quantify the performance of the proposed scheme, we derived closed form and asymptotic error probability expressions for Rayleigh/EW fading channels by considering instantaneous and mean-value power allocations. We further considered the primary-secondary interference and provided important design guidelines for practical CR RF-FSO systems. We believe that the proposed scheme will be useful for next generation wireless systems where a university student connected to an RF network wishes to use their home computer over the FSO path.

References

[1] A. Garhwal and P. P. Bhattacharya, "A survey on dynamic spectrum access techniques for cognitive radio," 2012, *arXiv:1201.1964*.

[2] S. Haykin, "Cognitive radio: Brain-empowered wireless communications," *IEEE J. Sel. Areas Commun.*, vol. 23, no. 2, pp. 201–220, Feb. 2005.

[3] E. Biglieri, A. J. Goldsmith, L. J. Greenstein, H. V. Poor, and N. B. Mandayam, *Principles of Cognitive Radio*. Cambridge, U.K.: Cambridge Univ. Press, 2013.

[4] J. Mitola and G. Q. Maguire, "Cognitive radio: Making software radios more personal," *IEEE Pers. Commun.*, vol. 6, no. 4, pp. 13–18, Aug. 1999.

[5] Q. Zhang, J. Jia, and J. Zhang, "Cooperative relay to improve diversity in cognitive radio networks," *IEEE Commun. Mag.*, vol. 47, no. 2, pp. 111–117, Feb. 2009.

[6] H. Li and Q. Zhao, "Distributed modulation for cooperative wireless communications," *IEEE Signal Process. Mag.*, vol. 23, no. 5, pp. 30–36, Sep. 2006.

[7] T. Q. Duong, D. B. da Costa, M. Elkashlan, and V. N. Q. Bao, "Cognitive amplify-and-forward relay networks over Nakagami-*m* fading," *IEEE Trans. Veh. Technol.*, vol. 61, no. 5, pp. 2368–2374, Jun. 2012.

[8] C. Zhong, T. Ratnarajah, and K.-K. Wong, "Outage analysis of decode-and-forward cognitive dual-hop systems with the interference constraint in Nakagami-*m* fading channels," *IEEE Trans. Veh. Technol.*, vol. 60, no. 6, pp. 2875–2879, Jul. 2011.

[9] J. Si, Z. Li, X. Chen, B. Hao, and Z. Liu, "On the performance of cognitive relay networks under primary user's outage constraint," *IEEE Commun. Lett.*, vol. 15, no. 4, pp. 422–424, Apr. 2011.

[10] D. Kedar and S. Arnon, "Urban optical wireless communication networks: The main challenges and possible solutions," *IEEE Commun. Mag.*, vol. 42, no. 5, pp. S2–S7, May 2004.

[11] M. Alzenad, M. Z. Shakir, H. Yanikomeroglu, and M.-S. Alouini, "FSO-based vertical backhaul/fronthaul framework for 5G+ wireless networks," *IEEE Commun. Mag.*, vol. 56, no. 1, pp. 218–224, Jan. 2018.

[12] M. A. Khalighi and M. Uysal, "Survey on free space optical communication: A communication theory perspective," *IEEE Commun. Surveys Tut.*, vol. 16, no. 4, pp. 2231–2258, Oct.–Dec. 2014.

[13] F. Demers, H. Yanikomeroglu, and M. St-Hilaire, "A survey of opportunities for free space optics in next generation cellular networks," in *Proc. IEEE 9th Annu. Commun. Netw. Serv. Res. Conf.*, 2011, pp. 210–216.

[14] B. Epple, "Simplified channel model for simulation of free-space optical communications," *J. Opt. Commun. Netw.*, vol. 2, no. 5, pp. 293–304, 2010.

[15] R. Barrios and F. Dios, "Exponentiated Weibull distribution family under aperture averaging for Gaussian beam waves," *Opt. Express*, vol. 20, no. 12, pp. 13055–13064, 2012.

[16] R. Barrios and F. Dios, "Exponentiated Weibull model for the irradiance probability density function of a laser beam propagating through atmospheric turbulence," *Opt. Laser Technol.*, vol. 45, no. 2, pp. 13–20, 2013.

[17] E. Zedini, I. S. Ansari, and M.-S. Alouini, "Performance analysis of mixed Nakagami-*m* and Gamma–Gamma dual-hop FSO transmission systems," *IEEE Photon. J.*, vol. 7, no. 1, Feb. 2014, Art. no. 7900120.

[18] L. Kong, W. Xu, L. Hanzo, H. Zhang, and C. Zhao, "Performance of a free-space-optical relay-assisted hybrid RF/FSO system in generalized $\mathcal{M}$-distributed channels," *IEEE Photon. J.*, vol. 7, no. 5, Oct. 2015, Art no. 7903319.

[19] B. Bag, A. Das, I. S. Ansari, A. Prokeš, C. Bose, and A. Chandra, "Performance analysis of hybrid FSO systems using FSO/RF-FSO link adaptation," *IEEE Photon. J.*, vol. 10, no. 3, Jun. 2018, Art no. 7904417.
[20] O. M. S. Al-Ebraheemy, A. M. Salhab, A. Chaaban, S. A. Zummo, and M.-S. Alouini, "Precise performance analysis of dual-hop mixed RF/unified-FSO df relaying with heterodyne detection and two IM-DD channel models," *IEEE Photon. J.*, vol. 11, no. 1, Feb. 2019, Art no. 7900522.
[21] J. Zhao, Shang-Hong, Wei-Hu, Y. Liu, and X. Li, "Performance of mixed RF/FSO systems in exponentiated Weibull distributed channels," *Opt. Commun.*, vol. 405, pp. 244–252, 2017.
[22] Y. Zhang, X. Wang, S.-H. Zhao, J. Zhao, and B.-y. Deng, "On the performance of 2 $\times$ 2 DF relay mixed RF/FSO airborne system over exponentiated Weibull fading channel," *Opt. Commun.*, vol. 425, pp. 190–195, 2018.
[23] Y. Wang, P. Wang, X. Liu, and T. Cao, "On the performance of dual-hop mixed RF/FSO wireless communication system in urban area over aggregated exponentiated Weibull fading channels with pointing errors," *Opt. Commun.*, vol. 410, pp. 609–616, 2018.
[24] H. Arezumand, H. Zamiri-Jafarian, and E. Soleimani-Nasab, "Outage and diversity analysis of underlay cognitive mixed RF-FSO cooperative systems," *J. Opt. Commun. Netw.*, vol. 9, no. 10, pp. 909–920, 2017.
[25] N. Varshney, A. K. Jagannatham, and P. K. Varshney, "Cognitive MIMO-RF/FSO cooperative relay communication with mobile nodes and imperfect channel state information," *IEEE Trans. Cogn. Commun. Netw.*, vol. 4, no. 3, pp. 544–555, Sep. 2018.
[26] N. Varshney and A. K. Jagannatham, "Cognitive decode-and-forward MIMO-RF/FSO cooperative relay networks," *IEEE Commun. Lett.*, vol. 21, no. 4, pp. 893–896, Apr. 2017.
[27] F. S. Al-Qahtani, A. H. A. El-Malek, I. S. Ansari, R. M. Radaydeh, and S. A. Zummo, "Outage analysis of mixed underlay cognitive RF MIMO and FSO relaying with interference reduction," *IEEE Photon. J.*, vol. 9, no. 2, Apr. 2017, Art no. 7902722.
[28] E. Erdogan, "On the performance of cognitive underlay RF/FSO communication systems with limited feedback," *Opt. Commun.*, vol. 444, pp. 87–92, 2019.
[29] V. N. Q. Bao, T. Q. Duong, and C. Tellambura, "On the performance of cognitive underlay multihop networks with imperfect channel state information," *IEEE Trans. Commun.*, vol. 61, no. 12, pp. 4864–4873, Dec. 2013.
[30] E. Erdogan, A. Afana, H. U. Sokun, S. Ikki, L. Durak-Ata, and H. Yanikomeroglu, "Signal space cognitive cooperation," *IEEE Trans. Veh. Technol.*, vol. 68, no. 2, pp. 1953–1957, Feb. 2019.
[31] K. Ho-Van, P. C. Sofotasios, G. C. Alexandropoulos, and S. Freear, "Bit error rate of underlay decode-and-forward cognitive networks with best relay selection," *J. Commun. and Netw.*, vol. 17, no. 2, pp. 162–171, 2015.
[32] E. Erdogan, "Joint user and relay selection for relay-aided RF/FSO systems over exponentiated Weibull fading channels," *Opt. Commun.*vol. 436, pp. 209–215, Apr. 2019.
[33] I. S. Ansari, S. Al-Ahmadi, F. Yilmaz, M.-S. Alouini, and H. Yanikomeroglu, "A new formula for the ber of binary modulations with dual-branch selection over generalized-k composite fading channels," *IEEE Trans. Commun.*, vol. 59, no. 10, pp. 2654–2658, Oct. 2011.
[34] I. S. Gradshteyn and I. M. Ryzhik, *Table of Integrals, Series, and Products*. New York, NY, USA: Academic, 2014.
[35] "From wolframresearch—The mathematical functions site," [Online]. Available: http://functions.wolfram.com
[36] A. M. Mathai, R. K. Saxena, and H. J. Haubold, *The H-function: Theory and Applications*. Berlin, Germany: Springer Science & Business Media, 2009.
[37] S. S. Ikki, "Optimisation study of power allocation and relay location for amplify-and-forward systems over Nakagami-m fading channels," *Trans. Emerg. Telecommun. Technol.*, vol. 25, no. 3, pp. 334–342, 2014.
[38] A. Afana, I. A. Mahady, and S. Ikki, "Quadrature spatial modulation in MIMO cognitive radio systems with imperfect channel estimation and limited feedback," *IEEE Trans. Commun.*, vol. 65, no. 3, pp. 981–991, Mar. 2017.
[39] J. A. Hussein, S. S. Ikki, S. Boussakta, and C. C. Tsimenidis, "Performance analysis of opportunistic scheduling in dual-hop multiuser underlay cognitive network in the presence of cochannel interference," *IEEE Trans. Veh. Technol.*, vol. 65, no. 10, pp. 8163–8176, Oct. 2015.